ORIGINAL ARTICLE

# Microstructure, growth banding and age determination of a primnoid gorgonian skeleton (Octocorallia) from the late Younger Dryas to earliest Holocene of the Bay of Biscay

**Sibylle Noé · Lester Lembke-Jene · Julie Reveillaud · André Freiwald**

**Abstract**  A fossil primnoid gorgonian skeleton (Octocorallia) was recovered on the eastern Galician Massif in the Bay of Biscay (NE Atlantic) from 720 m water depth. The skeleton shows a growth banding of alternating Mg–calcitic and organic (gorgonin) increments in the inner part, surrounded by a ring of massive fibrous calcite. Three calcite-dominated cycles, bounded by thick organic layers, consist of five light-dark couplets of calcite and gorgonin. Two AMS-^{14}C datings of the fossil skeleton give ages of 10,880 and 10,820 ± 45 ^{14}C years before present (BP). We arrive at a calibrated age range of 11,829–10,072 cal. years BP (two $\sigma$), which comprises the late Younger Dryas to the earliest part of the Holocene. The cyclic calcitic–organic growth banding may be controlled by a constant rate of calcite secretion with a fluctuating rate of gorgonin production, possibly related to productivity cycles. The skeletal fabric change of alternating calcitic–organic increments to massive fibrous calcite may be the result of hydrographic changes during the deglaciation as reflected by preliminary stable isotope data. If this hypothesis proves to be correct, primnoid gorgonians are able to match with varying hydrodynamic conditions by changing their biomineralisation mode.

S. Noé (✉) · L. Lembke-Jene
Leibniz Institute of Marine Sciences, IFM-GEOMAR,
Wischhofstr. 1-3, 24248 Kiel, Germany
e-mail: noe@pal.uni-erlangen.de

J. Reveillaud
Renard Centre of Marine Geology and Marine Biology Section,
Ghent University, Krijgslaan 281 S8, 9000 Gent, Belgium

*Present Address:*
S. Noé · A. Freiwald
Institute of Paleontology, University of Erlangen-Nuremberg,
Loewenichstr. 28, 91054 Erlangen, Germany

## Introduction

Modern deep-water primnoid gorgonians (Octocorallia) are quite common along the present-day Atlantic and Indo-Pacific oceans between 50 and 3,500 m depth (Heikoop et al. 2002; Andrews et al. 2002). Fossil specimens, in contrast, have been discovered only in few places so far. This may be a result of the metastable high-Mg calcite composing the skeletons (Sherwood et al. 2005a), which are prone to dissolution and diagenetic alteration.

During R/V Belgica's ''GALIPOR'' cruise (2004) off the Galician and Cantabrian continental margins, a fossil skeleton of the gorgonian family Primnoidae was recovered by a box core at the Massif Galicien de Í Est (sensu Le Danois 1948) from 720 m water depth (Fig. 1), corresponding to the deepest part of the NE Atlantic Central Water (McCartney 1992). Large parts of the primary skeletal structure are well preserved and allowed us to investigate the microstructure and growth banding and to determine an approximate age by radiocarbon dating. The skeleton may provide detailed insights into rapid changes of the hydrographic regime.

## Methods

The recovered skeleton was described and subsequently cross-cut into three slabs in the lab of IFM-GEOMAR. Sub-samples of 4.5 × 0.5 cm were taken for preparation of two highly polished petrographic thin sections of 25 μm

**Fig. 1** Topographic map of the study area. Location of primnoid skeleton recovered during R/V Belgicá s ''GALIPOR'' cruise (2004) from 720 m water depth is indicated
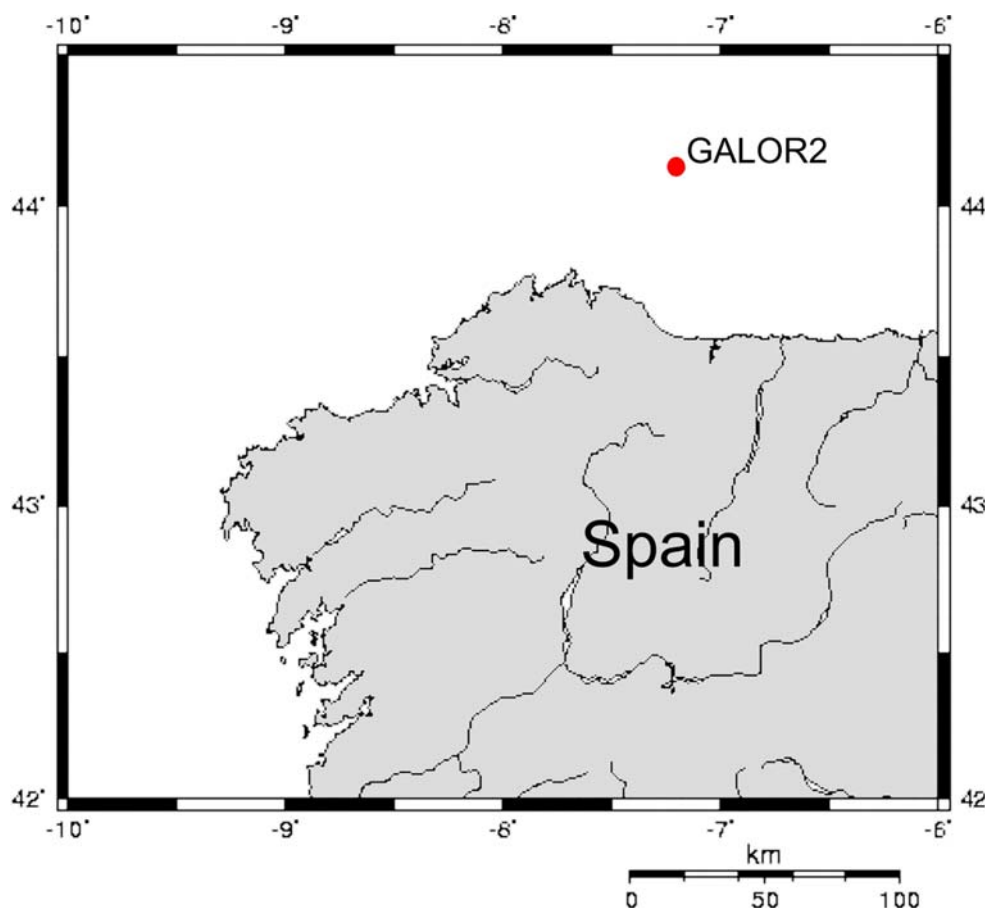
thickness applying normal and polarised transmitted light. Growth bands were counted in comparative studies on macroscopic (slabs) and microscopic (thin section) scales.

For an age determination, two samples were taken at the outer and inner margins of the primnoid trunk in a diagenetically unaltered area with a lateral record of 8.3 mm (Figs. 2c, 5). Samples were mechanically cleaned and inspected for eventually contaminating particles under a stereo microscope.

Conventional radiocarbon ages of the two samples were determined by the Leibniz Laboratory for Age Determination and Isotope Research, Kiel, according to the techniques outlined in Nadeau et al. (1998). AMS-$^{14}$C values were calibrated using the CALIB 5.0.1 program and the MARINE04 calibration dataset (Stuiver and Reimer 1993; Hughen et al. 2004).

Sub-samples for stable carbon and oxygen isotope analyses were drilled with a dentist drill of 500 µm radius along a cross-section of the skeleton and measured in the IFM-GEOMAR ISOLAB with a Finnigan MAT 252 isotope ratio mass spectrometer connected online to an automated CARBO KIEL II preparation unit. Calibration of the unit is maintained through NBS 19 and an internal laboratory standard (Solnhofen limestone), the long-term reproducibility of $\delta^{18}$O and $\delta^{13}$C is 0.06 and 0.04, respectively. All isotope values are referred to the Vienna-Pee Dee Belemnite Standard (‰ vs. V-PDB).

## Results

### Macrostucture

The primnoid skeleton represents part of the central growth axis of a primnoid coral colony, including a connected parallel lateral branch (Fig. 2a, b). The former, representing the trunk, measures 13 cm in length with a diameter of 2.0–3.2 cm and a thickness of 1 cm, while the latter measures 1.5 cm in diameter. The hollow skeletal axis is surrounded by concentric growth bands of alternating high-Mg calcite and organic matter consisting of the scleroprotein gorgonin (Heikoop et al. 2002; Sinclair et al. 2005). In cross-cut slabs, these tree-like increments with a thickness of 0.1–0.2 mm exhibit couplets of light, rigid calcite rings and dark, soft gorgonin-rich bands which is best exposed in slightly weathered areas (Fig. 2c). The outer part, on the other hand, appears massive, lacking a clear incremental fabric. The skeletal surface is strongly bioeroded

**Fig. 2** Fossil primnoid skeleton. **a–b** Lateral views of the skeleton showing the trunk and attached lateral branch. Growth increments are visible along the inner margin of the central axis. **c** Vertical view of the cross-cut skeleton. Varying thickness of skeleton is due to bioerosion. Note the difference between the well-preserved, compact areas and the diagenetically altered zones revealing the growth banding of elevated calcitic increments (*light*) and weathered organic layers (*dark*). **d** Surface of the primnoid skeleton showing numerous borings and an encrusting serpulid worm tube (*arrow*)
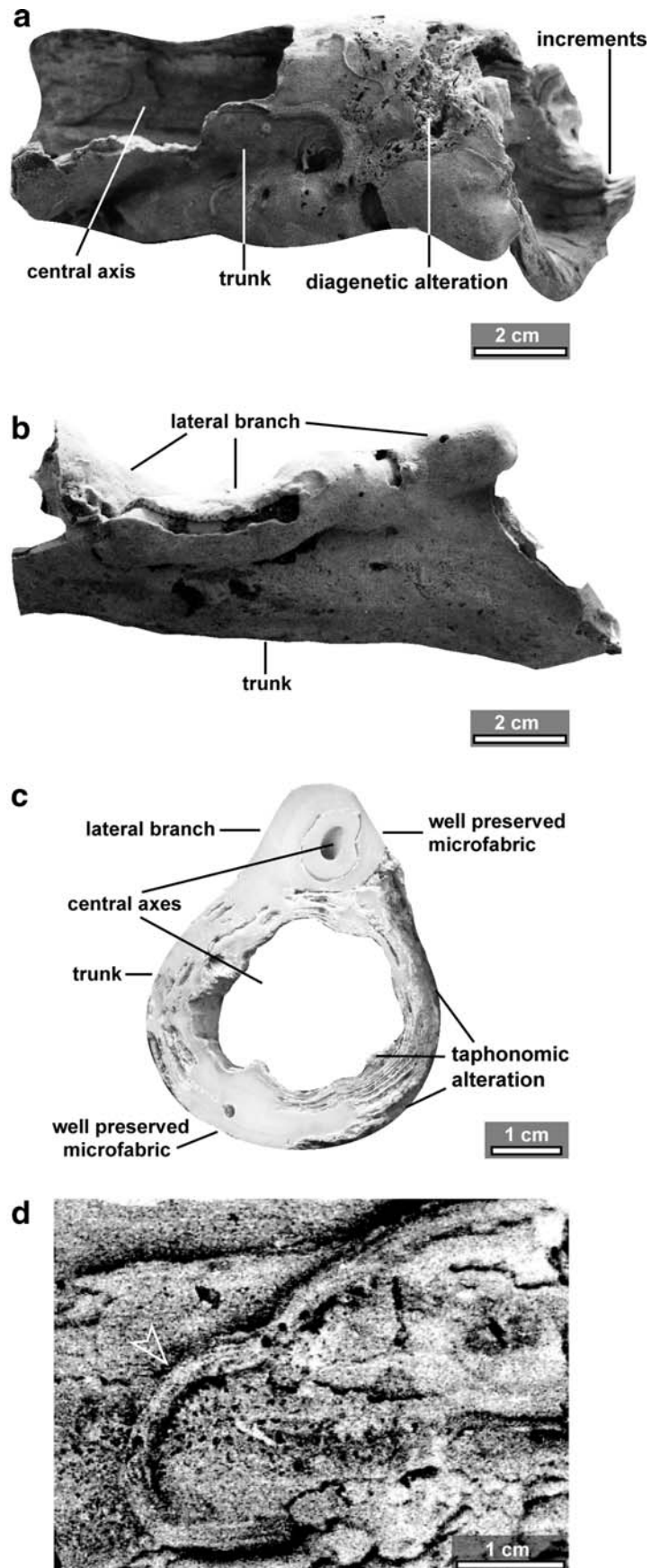
down to 4 mm depth and encrusted by serpulid worm tubes and bryozoans (Fig. 2d).

## Microstructure

Cross-cut slabs of the trunk and lateral branch exhibit two microfabrics in thin sections: an inner zone composed of an alternation of high-Mg–calcitic and organic increments (Fig. 4e, lower and central part of image) which constitutes a primnoid-typical growth banding (Grasshoff and Zibrowius 1983; Heikoop et al. 2002; Risk et al. 2002; Sherwood et al. 2005a), and an outer zone of massive fibrous calcite (Fig. 4e, upper part). In spite of the locally blurred boundary between both zones, there is no evidence of a growth interruption such as bioerosion or of early-diagenetic dissolution. X-ray diffraction gave a uniform high-Mg–calcite mineralogy without relevant indications of low-Mg calcite or other, diagenetically induced carbonate phases.

## Inner zone

The inner skeletal part measures 5–7.5 mm in thickness in the section of increment counts (Figs. 2c, 5). It consists of alternating calcitic and organic increments. While the dominating calcite layers form the skeletal framework, thick organic interlayers are intercalated at cyclic intervals (Figs. 3b and 4e). The basic fabric of the calcite increments is characterised by radial to divergent-radial fibrous crystals. In radial arrangement fibrous crystals build isopachous layers of a largely uniform thickness (Fig. 3c–g). Divergent-radial crystals, on the other hand, are assembled in fibrous arrays or 40–60-μm-thick fan-shaped ''fascicles'' (Cohen and McConnaughey 2003), which may have fused laterally with adjacent fans to form highly wavy layers (Fig. 3a, b, d, e). The fascicles are commonly lined by gorgonin seams (Fig. 3a, b). Individual fibrous crystals of 10 μm length are hard to distinguish as they grew in optical continuity with each other, causing a swinging extinction across the layers (Fig. 3e, f).

Calcite layers show two types of alternating crystal fabrics: (1) inclusion-rich layers with a light to dark-brown colour, depending on the percentage and size of gorgonin inclusions (Fig. 3a–g); the 100–120-μm-thick layers show fine internal laminations as a result of crystal generations growing in optical continuity upon each other, separated by dark organic films (Fig. 3c, d); (2) inclusion-poor layers of translucent crystals with a thickness of 30–40 μm, consisting of a single crystal generation (Fig. 3a–e, g).
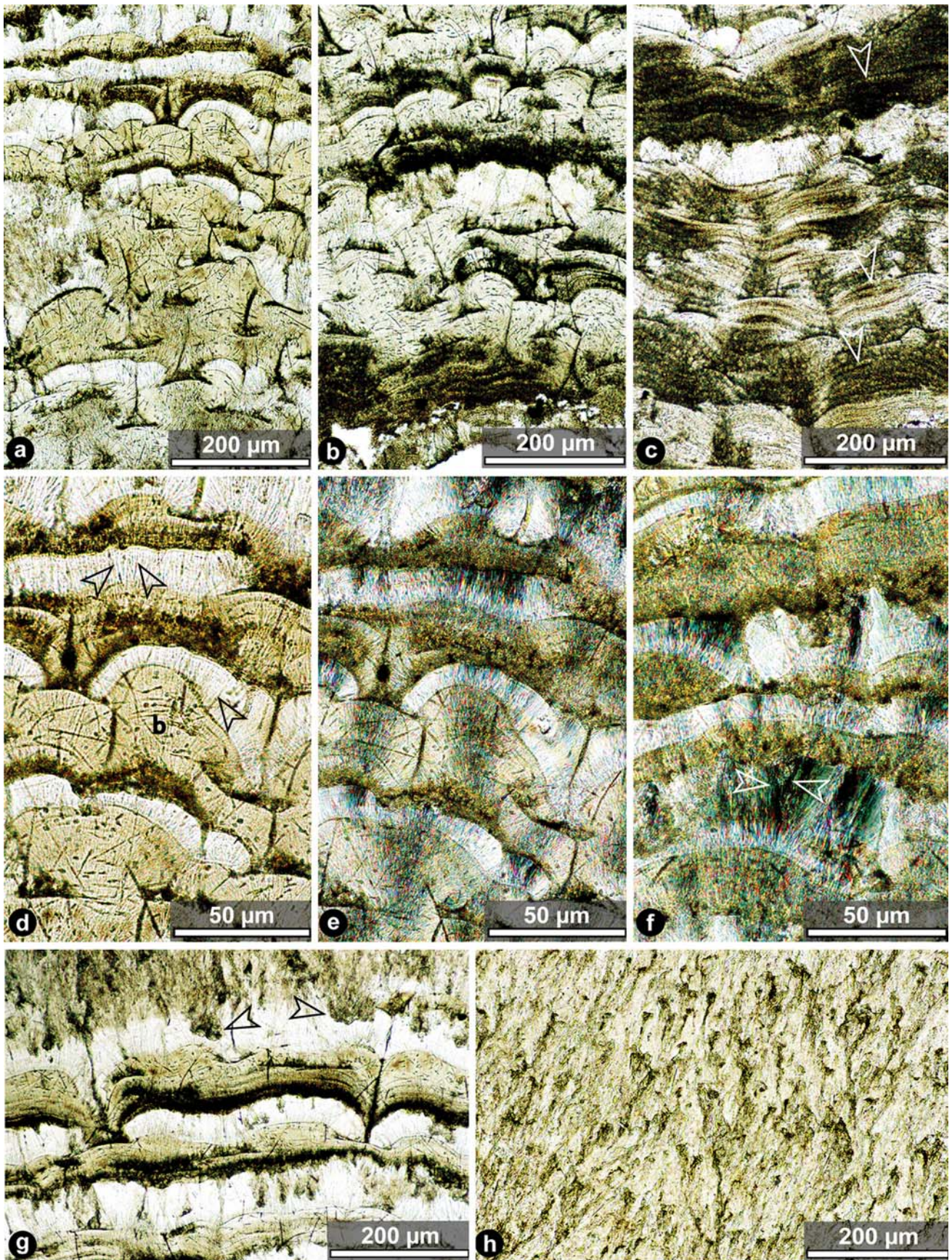
Organic layers also represent two types: (1) 30-μm-thin, discontinuous layers which are predominantly restricted to seams surrounding the calcitic fascicles (Fig. 3a, b, d) and may locally disintegrate to patches, causing a fine internal banding on microscale (Fig. 3b, g); (2) 100–120-μm-thick
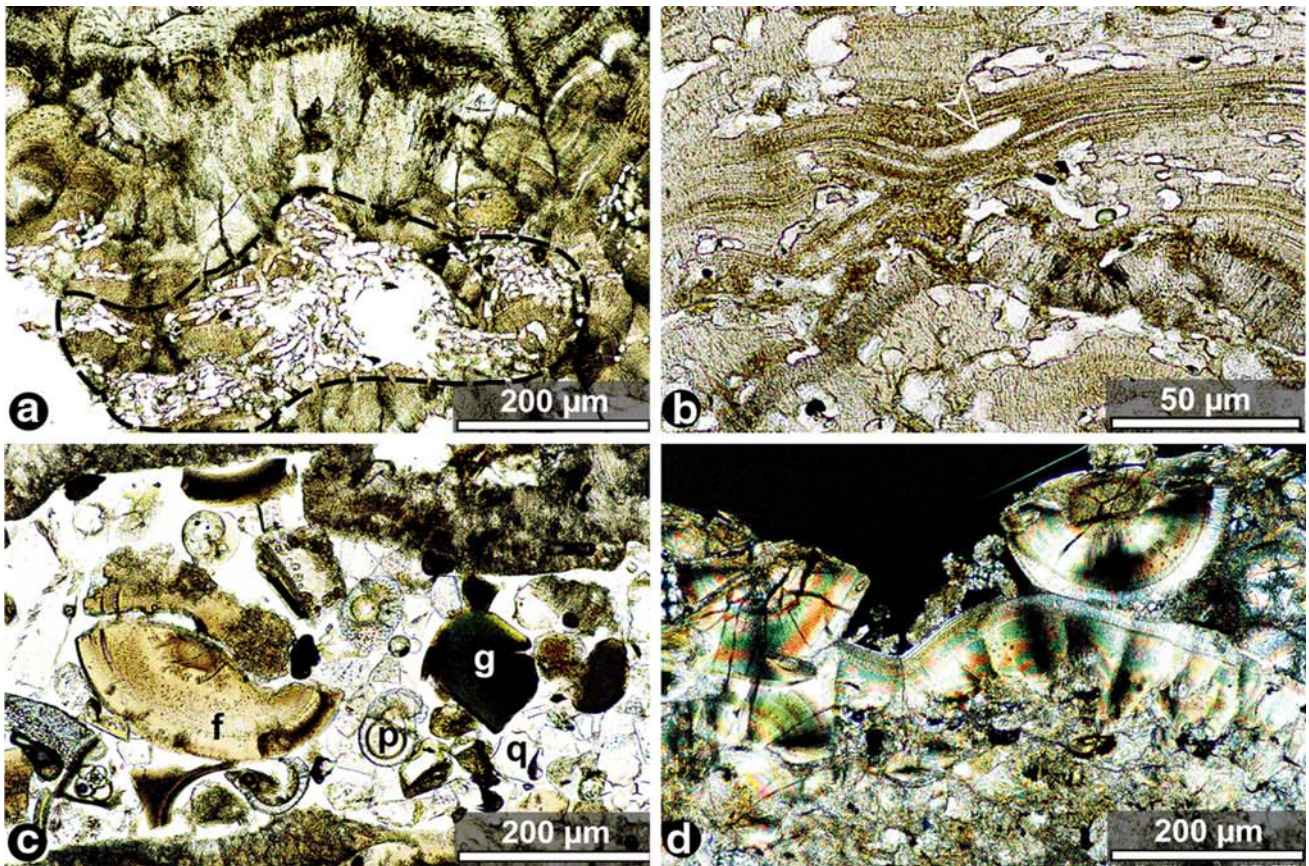
**Fig. 3** Primary microfabric of the primnoid skeleton (petrographic thin sections in transmitted light). **a** Alternation of inclusion-rich divergent-radial fascicle layers (*ochre* to *creamy*) and inclusion-poor radial-fibrous crystal layers (*light*) in the calcitic–organic alternation. Note organic linings atop the fascicles. Plane-polarised light. **b** Calcitic–organic growth banding showing interconnected fascicles of inclusion-rich crystals, thin inclusion-poor calcite layers, thin discontinuous organic layers and linings, and a thick organic-rich layer (*base*) marking the base of the oldest cycle. Dark layers in the *centre* elucidate the inhomogeneous distribution of gorgonin, responsible for their discontinuity. Plane-polarised light. **c** Organic-rich part of the calcitic–organic alternation in *left* part of slab. Note inclusion-rich calcite layers in the *centre* and individual crystal generations in the organic-rich layers (*arrows*). Plane-polarised light. **d** Close-up of calcitic–organic growth banding. Note fan-shaped fabric of inclusion-rich layers (*centre*), individual crystals in the light radial to divergent-radial fibrous layers (*arrows*), spot-wise enrichment of gorgonin inclusions along the fascicle boundaries marking thin discontinuous organic layers, and abundant microborings dissecting the fascicles (**b**). Plane-polarised light. **e** Same image as in **d** in cross-polarised light showing the swinging extinction in both calcite types. **f** Alternation of inclusion-rich (*brownish*) and inclusion-poor fibrous calcite layers (*light* to *dark grey* depending on extinction position). Note slight divergence of individual crystals in the lowermost inclusion-poor layer (*arrows*). Cross-polarised light. **g** Transition from the calcitic–organic alternation of the inner zone to massive fibrous calcite of the outer zone (*top*). Note somewhat blurred boundary with fibrous crystals cutting into the light calcite layer underneath (*arrows*). Plane-polarised light. **h** Fibrous fabric composing the outer part of the skeleton. Note fibrous crystals being arranged in bundles and surrounded by organic seams. Plane-polarised light

continuous layers that form macroscopic growth bands (Figs. 3c, 4e). Thin sections show a mixed organic–calcitic nature representing a variation of the radial fibrous calcite crystals with a very high percentage of gorgonin inclusions. The mixed organic–calcitic composition is supported by the fine laminations at a 10 μm scale observed in the dark layers, which mimics that of the inclusion-rich calcite layers (Fig. 3b, c). This composition corresponds to that of modern primnoids, in which the dark couplets contain a higher percentage of gorgonin compared to calcite (Risk et al. 2002).
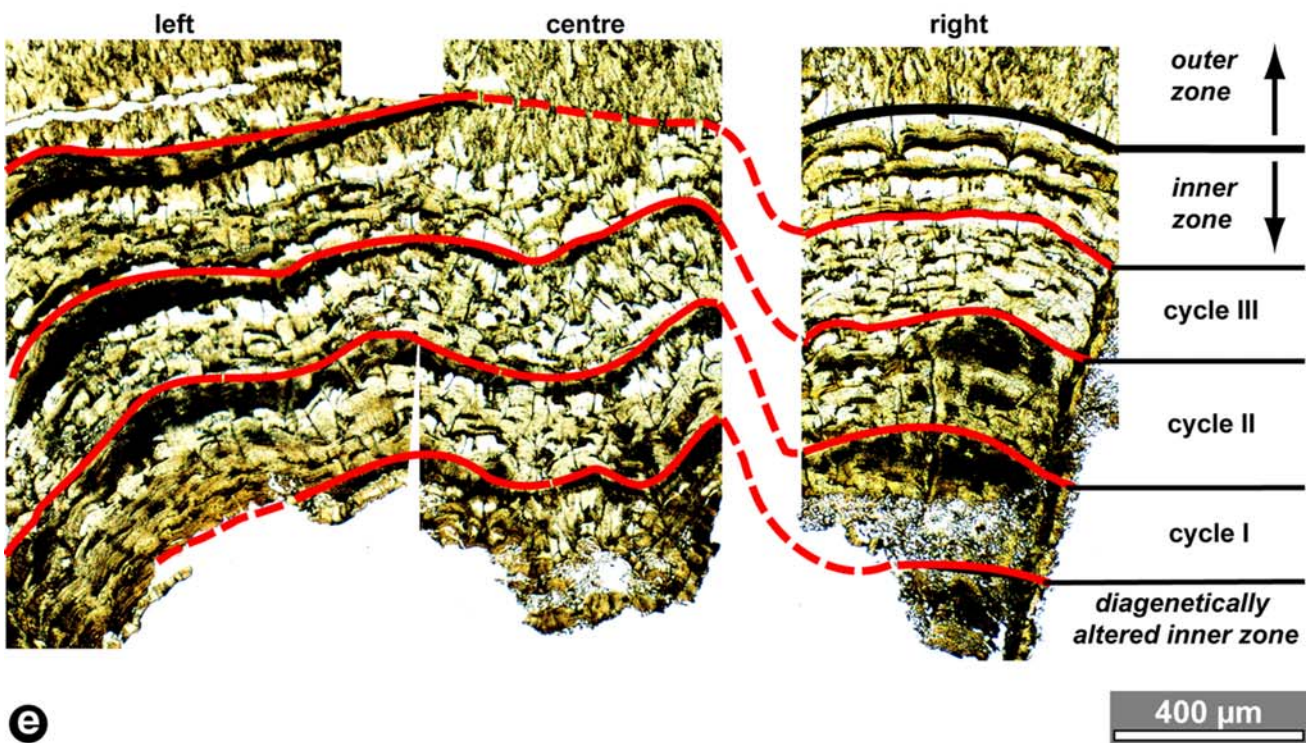
## Outer zone

The compact outer zone of the trunk and lateral branch with an average thickness of 2.5 mm (Fig. 5) consists of divergent-radial fibrous calcite crystals of 10–12 μm length, which are arranged in bundles and fans that interfinger in three dimensions. The individual fibres are surrounded by thin organic (gorgonin) seams that are responsible for the cloudy appearance in thin sections (Fig. 3h). This composition and fabric corresponds to that of isidid gorgonians (Noé and Dullo 2006). The somewhat blurred boundary to the calcitic–organic alternation of the inner zone (Figs. 3g and 4c) is a primary feature, caused by slightly varying rates of calcite versus gorgonin secretion by the individual polyps of the coral colony.

200 µm

50 µm

200 µm

200 µm

Photomosaic

left                    centre                    right

outer zone

inner zone

cycle III

cycle II

cycle I

diagenetically altered inner zone

400 µm

◀ **Fig. 4** Taphonomic features on the primnoid skeleton (petrographic thin sections in transmitted light) and photomosaic of a cross-section. **a** Fungal borings in a fascicle layer of the inner skeletal zone, starting from a bivalve boring (surrounded by *black dotted line*). Plane-polarised light. **b** Close-up of dissolution-enlarged fungal borings in the calcitic–organic alternation of the inner zone, being mostly restricted to the calcitic layers. Note vug being elongated parallel to lamination in organic-rich calcite layers (*arrow*). Plane-polarised light. **c** Bivalve boring filled with planktonic foraminifers (*p*), glauconite grains (*g*), detrital quartz (*q*) and broken fascicles derived from the inner zone of skeleton (*f*). Plane-polarised light. **d** Diagenetically altered zone along a bivalve boring. Note radial-fibrous cement overgrowth (*white seams*) on fascicles showing a swinging extinction. Cross-polarised light. **e** Photomosaic showing growth banding in the *left* and *right* halves of the skeletal cross-section in plane-polarised light. Note primnoid-typical growth banding of inclusion-rich (*grey*) and inclusion-poor calcite layers (*light*) alternating with organic-rich layers (*dark*) of the inner zone, and irregular transition to the outer zone of fibrous calcite (*top*)

Taphonomic alteration

After decay of the coral tissue surrounding the central axis, the outer and inner margins of the central axis were locally affected by bioerosion which resulted in a weakening of the skeleton and a partial breakdown of the growth bands at these sites (Fig. 2a, c). In addition, preferential decay of the organic interlayers in the inner zone resulted in breakdown of the surrounding calcitic bands and thus in an enlargement of the central tube (Grasshoff and Zibrowius 1983).

Microbial activity: besides numerous micritised microborings that pierce the skeleton throughout (Fig. 3a, b, d, e), certain areas show a somewhat vesicular structure which is the result of fungal boring activity and combined release of carbonic and humic acids causing carbonate dissolution (Fig. 4a, b). The resulting solution-enlarged vugs are predominantly restricted to the organic-poor layers (Fig. 4a), since gorgonin inclusions represent natural barriers towards the dissolution pathways. Hence, some elongated vugs occurring in the organic-rich layers are oriented parallel to the lamination (Fig. 4b). Microbial micritisation along the outer margin of the skeleton resulted in a loss of the original microstructure and produced an indistinct peloidal to microgranular fabric (Fig. 4d).

Macroborings: sponge and bivalve borings cutting into the skeleton are filled with planktonic foraminifers, detrital quartz, glauconite grains, and calcitic fascicles, the latter

**Fig. 5** Cross-section of the skeleton showing the boundary between the inner and outer zone, calcitic–organic increments, profiles of increment counts, and sampling sites. The two *lines* indicating the zone of ''increment counts on thin section photomosaic'' enclose the area of growth band counts along several traverses. Slab image is modified by high-pass filter
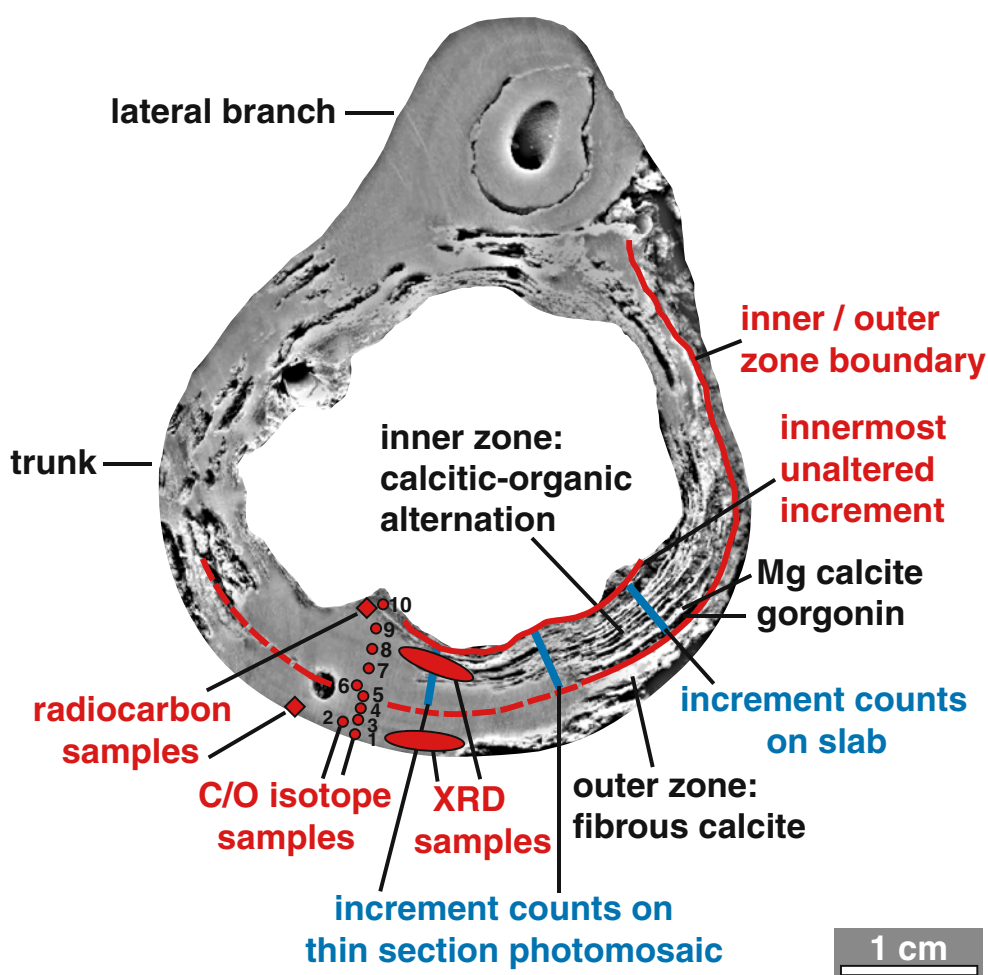
being bioerosion relicts of inclusion-rich fibrous calcite bands (Fig. 4c). Fascicle fragments may show isopachous radial-fibrous cement overgrowths which precipitated during early diagenesis (Fig. 4d).

Growth banding pattern

Growth band counting, in combination with absolute age determination, provides information on the age record of the fossil primnoid skeleton. On macroscale, increments were counted on a cross-cut slab (Fig. 5). A thin-section photomosaic served for counting on microscale (Fig. 4e; see Fig. 5 for position).

Macroscale: the slab image modified by high-pass filter reveals 30 bands of alternating light calcitic and dark organic layers in the inner zone with a highly variable thickness. The outer zone of fibrous calcite appears largely homogenous due to the lack of a calcitic–organic or colour banding pattern.

Microscale: the thin-section photomosaic (Fig. 4e) shows three parts of a larger mosaic: the ''left'' and ''centre'' parts are connected, while the ''right'' part is shifted 1 cm towards the right (see Fig. 5 for location). The hollow central axis with the innermost, partially bioeroded and diagenetically altered part is shown at the base here, while a small part of the outer fibrous zone is shown on its top. The inner zone exhibits a quite irregular alternation of inclusion-rich and inclusion-poor calcite layers and intercalated organic layers. Conspicuous lateral microfabric changes are observed across the photomosaic: while slightly wavy calcite layers with abundant, irregularly distributed organic enrichments dominate in the left part, dome-shaped fascicles with a minor percentage of organic inclusions compose the layers in the right part. On a mesoscale, lateral changes are documented by a thicker calcitic–organic alternation at the right part and a thinner one in the central part due to a cut-in of the outer fibrous calcite.

Three major cycles with a slightly varying thickness are recognised in the inner zone of the photomosaic (Fig. 4e). They are bounded by continuous organic layers which are thinning towards the right in the left and central part or towards the left in the right part, respectively. The individual cycles are composed of calcitic–organic couplets, whereas the gorgonin is enriched on top of and in the pore space between the calcitic fascicles, producing a somewhat mottled fabric rather than a regular layering. In some areas, a thick translucent calcite layer occurs beneath the topmost organic layer. Due to the discontinuity of these thin organic bands, cross-sections differ from one another, which required a growth band counting along several traverses from left to right. Increment counts consistently gave ten individual layers of inclusion-rich or inclusion-poor calcite and gorgonin, i.e. five light–dark couplets in each cycle. Hence the three cycles consist of 30 bright and dark bands, corresponding to the number counted in the slab profile.

Radiocarbon dating

Conventional AMS-^{14}C datings gave an age of 10,880 ± 45 years before present (BP) for the inner margin analysis and 10,820 ± 45 years BP for the outer margin (Table 1), which corresponds to the termination of the Younger Dryas and to the earliest Holocene. The difference between inner and outer margin amounts to 60 ± 67 years. This difference is too small, however, for a statistically significant corroboration of the count results.

For transferring the conventional ^{14}C ages into calibrated calendar years, we used a reservoir effect (R) of 408 years in line with previous data (Hughen et al. 2004; Robinson et al. 2005) and tacitly assumed that R remained constant during the Younger Dryas and earliest Holocene, though this assumption may well be not valid (Robinson et al. 2005; Waelbroeck et al. 2001). We applied no further local surface water reservoir age (ΔR) correction for the samples: the modern mixed layer reservoir age in the region averages between 20 and 22 years and is thus negligible (Harkness 1983; Broecker and Olson 1961). In order to get meaningful age control, however, one also has to subtract the age of the regional bottom water mass of the coral site from the measured conventional ^{14}C age before calibration. In fact, assigning a ventilation age proves to be difficult. In a previous work on deep-water corals using paired U/Th and AMS-^{14}C data, best estimates range widely between 650 ± 190 and 1,485 ± 330 years for comparable time periods and water depths (Schröder-Ritzrau et al. 2003, Samples 654, 660, 2307, and 2631). Hence, we subtracted an average value of 1,000 years with a rather large uncertainty of ±500 years from our values.

These large uncertainties, mainly caused by the determination of the local surface water reservoir age and the ventilation age of the bottom water surrounding the coral

**Table 1** AMS-^{14}C original data and calibrated ages

| Lab. code | Conventional age ^{14}C yr | Uncertainty yr | 1 sigma age range cal. yr BP | 2 sigma age range cal. yr BP |
|---|---|---|---|---|
| KIA 29464 inn. | 10,880 | 45 | 10,323–11,829 | 9,794–12,641 |
| KIA 29465 aus. | 10,820 | 45 | 10,072–11,571 | 9,486–12,318 |

site, result in a wide range of ages for the specimen, encompassing the Younger Dryas and Early Holocene. Taking preliminary considerations and the derived one sigma age range at face value, one may assume that the specimen lived during Termination Ib or during the deglacial in the earliest part of the Holocene, i.e. 11,829–10,072 cal. years BP. Table 1 shows the conventional $^{14}$C data and the calibrated ages.

Future studies (U/Th dating) will help to constrain the absolute age and give valuable information about past water-mass ventilation ages in the Gulf of Biscay during the deglaciation. These data will allow the constraining of estimates for the lateral linear extension rates of the skeleton and the verification as to whether the calcitic–organic cycles composed of five light–dark couplets represent annual bands by analogy to modern primnoid skeletons (Heikoop et al. 2002; Risk et al. 2002; Andrews et al. 2002; Sherwood et al. 2005b, c).

Stable oxygen and carbon isotopes

In order to assess the controls of the growth-banding pattern of the octocoral skeleton, stable oxygen and carbon isotopes were measured. Ten sub-samples were taken in a cross-section of the slab. In the growth profile (Fig. 6a), the boundary between the inner zone (left part of the *x*-axis) and outer zone (right part) is located at 6.8 mm distance.

The $\delta^{18}$O values range between 2.1–2.6‰ versus V-PDB and show relatively low scatter within the measured profile (Fig. 6a). If we assume that primnoid gorgonians incorporate oxygen isotopes anywhere close to equilibrium, as is known for other deep-water corals (Smith et al. 1997; Adkins et al. 2003), the absolute values would rather imply an Early Holocene age of the specimen, as indicated by a quick comparison with published values of $\delta^{18}$O for intermediate water masses in the region (e.g. Labeyrie et al. 1992; Smith et al. 1997). We also observe a slight trend to heavier values in the outer growth zone from 2.1 to 2.6‰. The difference of 0.5‰ might imply a short-term change in the temperature–salinity characteristics in intermediate waters of roughly 2°C or any combination thereof accordingly, recorded during the coral's life span.

The $\delta^{13}$C values fluctuate in a small range between –1 and +0.26‰ versus V-PDB, i.e. the values are likely depleted with respect to $\delta^{13}C_{\sum CO2}$. The paired $\delta^{13}$C/$\delta^{18}$O data (Fig. 6b) show a positive correlation of both isotopes with a regression line of 0.65, which is significantly worse than paired stable isotope data in scleractinians. Nevertheless, this might indicate ''vital effects'', for example kinetic fractionation processes, comparable with other deep-water coral skeletons with different carbonate phases (e.g. aragonite). The low variability of $\delta^{13}$C with approximately 1‰ compared to a range of up to 10‰ measured in scleractin-

ians (e.g. Smith et al. 1997; Adkins et al. 2003), shows that kinetic controls on the fractionation may play a dominant role rather than metabolic ones in comparison with scleractinians (McConnaughey 1989; Adkins et al. 2003).

# Discussion

Controls on growth banding

The inner zone of the fossil primnoid skeleton on macroscale shows a regular alternation of calcitic and organic bands. On microscale, however, the thick organic bands marking cycle boundaries are thinning laterally, while the thin organic-rich seams, as parts of the light–dark couplets composing the cycles, are quite discontinuous in that they pinch out laterally and locally show a patchy distribution between individual calcitic fascicles.

A possible control of the varying thickness and continuity of the organic layers in the calcitic–organic alternation may be a largely constant rate of enzymatically controlled secretion of calcite, overprinted by a fluctuating rate of gorgonin production. The latter depends on the supply of sinking particulate organic matter and/or zooplankton which *Primnoa* preferentially feeds on (Griffin and Druffel 1989; Sherwood et al. 2005c). These nutrients, derived from the surface water and sinking through the water column to the coral site, were consumed by the coral polyps and used as carbon source for the protein biosynthesis of the coral tissue and of skeleton-forming gorgonin (Heikoop et al. 1998, 2002). By analogy with modern primnoids, the cycle-bounding organic layers may be triggered by productivity cycles in the surface water, responsible for a cyclically increased gorgonin production.

Percentages of organic inclusions in the calcitic bands of the inner zone may vary laterally within one layer. This irregular distribution is a primary feature, since in the case of a diagenetic redistribution, the organic matter would not mimic the lamination of the inclusion-rich calcite layers but rather cut through individual growth bands. Since the coral colony surrounds the entire skeletal axis and growth interruptions were not observed in the skeleton, it is unlikely that the organic inclusions consisting of particulate organic matter became incorporated into the growing calcite crystals.

Further $\delta^{13}C_{org}$ and $\delta^{15}$N analyses are required to check if the composition of these organic inclusions in the calcite layers corresponds to that of the organic bands. Organogeochemical analyses should elucidate if both types of organic products derived from different carbon sources, which were consumed by the coral and metabolised via different biochemical pathways, thus resulting in different end-products.

**Fig. 6** Stable carbon and oxygen isotope diagrams. **a** Profile of skeletal cross-section shown in Fig. 5, based on ten values. The profile runs from the inner margin (1 mm distance) to the outer margin (10 mm distance). The boundary between the inner and outer growth zone is located at 6.8 mm distance corresponding to sample five in Fig. 5. **b** Scatter plot of $\delta^{18}O$ versus $\delta^{13}C$
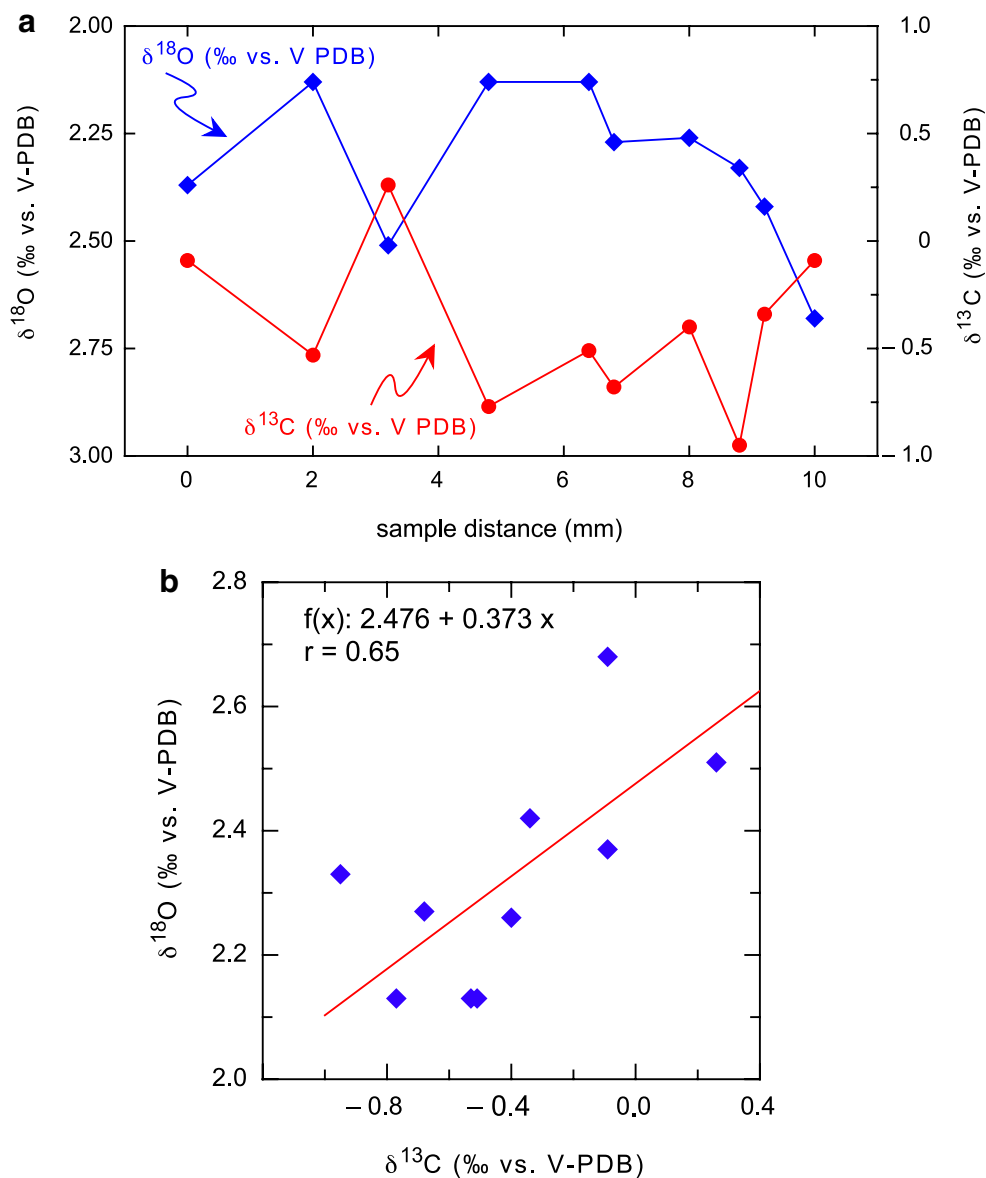


### Change of growth fabric

The ultimate controls of the conspicuous change from a calcitic–organic alternation of the inner zone to a massive fibrous Mg–calcite of the outer zone enveloping the central axis are not known. In general, the enzymatically controlled secretion of calcareous crusts around the skeletal axis requires less energy than the biosynthesis of the scleroprotein gorgonin, as dissolved inorganic carbon (DIC) is not limited in the seawater above the lysocline; hence, the formation of crusts is a common phenomenon in gorgonian skeletons.

Grasshoff and Zibrowius (1983) observed a great variety of calcareous crusts on skeletal axes of several gorgonian families including the Primnoidae: crusts may be present or

absent on diverse specimens of the same species. Hence an ontogenetic control on secretion of carbonate crusts around gorgonian skeletal axes during late-stage growth is unlikely. According to Grasshoff and Zibrowius (1983), a horny axis providing flexibility of the skeleton enables the coral colony to grow in areas of high hydrodynamic energy. On the other hand, calcareous crusts which are responsible for stability preferentially form in deeper water areas of reduced water energy.

Another conceivable environmentally controlled scenario, referring to the hydrodynamic regime of our Biscay primnoid specimen, is that during the juvenile growth stage of the thin central axis, high flexibility, provided by gorgonin, was required to enable skeletal growth in that current-affected continental margin regime. In this case,

sufficient organic nutrient supply enables the protein biosynthesis of the gorgonin layers. After the adult branched skeletal axis had reached a specific size and thickness, stability of the skeleton may have played a major role in survival under increasing hydrodynamic energy conditions, which consequently resulted in a preferential secretion of massive calcitic increments around the skeletal axis.

A similar formation of calcareous crusts was observed in a highly branched Mid-Holocene isidid gorgonian skeleton from the southern slope of Chatham Rise (New Zealand), where the secretion of organic nodes which vertically alternate with Mg–calcitic internodes ceased simultaneously in all branches as a result of a growth interruption triggered by an extrinsic event. After the recovery of coral growth which was linked with an increase of current energy, the colony continuously accreted increments of fibrous calcite around the skeleton, characterising the late-stage skeletal growth (Noé and Dullo 2006).

The transition from the Younger Dryas to the deglacial period of the earliest Holocene was linked to changes of the intermediate water circulation and thus of the hydrographic regime (Berger and Jansen 1995). An increase of hydrodynamic energy such as vigorous contour currents affecting the continental slope at the depth of the coral site might have triggered the secretion of massive fibrous calcite which envelopes the more flexible calcitic–organic cycles of the older skeleton, thus providing the required skeletal rigidity.

In addition, changing hydrologic conditions might have influenced the surface water productivity and particulate organic matter flux as indicated by our $\delta^{13}$C profile. A reduced rate of organic particle supply and thus of gorgonin production might result in the secretion of a massive crust of fibrous calcite crystals around the calcitic–organic alternation of the inner skeleton. For this calcite precipitation, metabolically generated carbon dioxide is used, together with a continuous uptake of dissolved inorganic carbon from the ambient bottom water (Lucas and Knapp 1997). These preliminary results support the hypothesis that long-lived primnoid octocoral colonies, by analogy with isidid gorgonians, may be able to change their mode of biomineralisation according to changing hydrographic conditions.

## References

Adkins JD, Boyle EA, Curry WB, Lutringer A (2003) Stable isotopes in deep-sea corals and a new mechanism for ''vital effects''. Geochim Cosmochim Acta 67:1129–1143

Andrews AH, Cordes EE, Mahoney MM, Munk K, Coale KH, Cailliet GM, Heifetz J (2002) Age, growth and radiometric age validation of a deep-sea, habitat-forming gorgonian (*Primnoa resedaeformis*) from the Gulf of Alaska. Hydrobiologia 471:101–110

Berger WH, Jansen E (1995) Younger Dryas episode: ice collapse and superfjord heat pump. In: Troelstra SR, van Hinte JE, Ganssen GM (eds) The Younger Dryas. North-Holland, Amsterdam, pp 61–105

Broecker WS, Olson EA (1961) Lamont radiocarbon measurements VIII. Radiocarbon 3:176–204

Cohen AL, McConnaughey TA (2003) A geochemical perspective on coral mineralization. In: Dove M, Weiner S, de Yoreo J (eds) Biomineralization. Rev Miner Geochem 54:151–187

Grasshoff M, Zibrowius H (1983) Kalkkrusten auf Achsen von Hornkorallen, rezent und fossil (Cnidaria, Anthozoa, Gorgonaria). Senckenbergiana marit 15:111–145

Griffin SM, Druffel ERM (1989) Sources of carbon to deep-sea corals. Radiocarbon 31:533–543

Harkness DD (1983) The extent of the natural $^{14}$C deficiency in the coastal environment of the United Kingdom. J Eur Study Group Phys Chem Math Tech Appl Archaeol PACT 8(IV.9):351–364

Heikoop JM, Risk MJ, Lazier AV, Schwarcz HP (1998) $\delta^{13}$C and $\delta^{18}$O of a deep-sea gorgonian coral from the Atlantic coast of Canada. EOS 79(17):179

Heikoop HM, Hickmott DD, Risk MJ, Shearer CK, Atudorei V (2002) Potential climate signals from the deep-sea gorgonian coral *Primnoa resedaeformis*. Hydrobiologia 471:117–124

Hughen KA, Baillie MGL, Bard E, Beck JW, Bertrand CJH, Blackwell PG, Buck CE, Burr GS, Cutler KB, Damon PE, Edwards RL, Fairbanks RG, Friedrich M, Guilderson TP, Kromer B, McCormac G, Manning S, Ramsey CB, Reimer PJ, Reimer RW, Remmele S, Southon JR, Stuiver M, Talamo S, Taylor FW, van der Plicht J, Weyhenmeyer CE (2004) Marine radiocarbon age calibration, 0–26 cal kyr BP. Radiocarbon 46:1059–1086

Labeyrie LD, Duplessy J-C, Duprat J, Juillet-Leclerc A, Moys J, Michel E, Kallel N, Shackelton NJ (1992) Changes in vertical structure of the North Atlantic Ocean between glacial and modern times. Quaternary Sci Rev 11:401–413

Le Danois ED (1948) Les profondeurs de la mer. Payot, Paris, 303 pp

Lucas JM, Knapp LW (1997) A physiological evaluation of carbon sources for calcification in the octocoral *Leptogorgia virgulata* (Lamarck). J Exp Biol 200:2653–2662

McCartney MS (1992) Recirculating components to the deep boundary current of the northern North Atlantic. Prog Oceanogr 29:283–383

McConnaughey T (1989) $^{13}$C and $^{18}$O isotopic disequilibrium in biological carbonates: I. patterns. Geochim Cosmochim Acta 53:151–162

Nadeau MJ, Grootes PM, Schleicher M, Hasselberg P, Rieck A, Bitterling M (1998) Sample throughout and data quality at the Leibniz-Labor AMS facility. Radiocarbon 40(special issue):239–245

Noé SU, Dullo W-Chr (2006) Skeletal morphogenesis and growth mode of modern and fossil deep-water isidid gorgonians (Octocorallia) in the West Pacific (New Zealand and Sea of Okhotsk). Coral Reefs 25:303–320

Risk MJ, Heikoop JM, Snow MG, Beukens R (2002) Lifespans and growth patterns of two deep-sea corals: *Primnoa resedaeformis* and *Desmophyllum cristagalli*. Hydrobiologia 471:125–131

Robinson LF, Adkins JF, Keigwin LD, Southon J, Fernandez DP, Wang S-L, Scheirer DS (2005) Radiocarbon variability in the western North Atlantic during the last deglaciation. Science 310:1469–1473

Schröder-Ritzrau A, Mangini A, Lomitschka M (2003) Deep-sea corals evidence periodic reduced ventilation in the North Atlantic during the LGM/Holocene transition. Earth Planet Sci Lett 216:399–410

Sherwood OA, Heikoop JM, Sinclair DJ, Scott DB, Risk MJ, Shearer C, Azetsu-Scott K (2005a) Skeletal Mg/Ca in *Primnoa resedaeformis*: relationship to paleotemperature? In: Freiwald A, Roberts JM (eds) Cold-water corals and ecosystems. Springer, Heidelberg, pp 1061–1079

Sherwood OA, Scott DB, Risk MJ, Guilderson TP (2005b) Radiocarbon evidence for annual growth rings in the deep-sea octocoral *Primnoa resedaeformis*. Mar Ecol Prog Ser 301:129–134

Sherwood OA, Heikoop JM, Scott DB, Risk MJ, Guilderson TP, McKinney RA (2005c) Stable isotope composition of deep-sea gorgonian corals *Primnoa* spp.: a new archive of surface processes. Mar Ecol Prog Ser 301:135–148

Sinclair DJ, Sherwood OA, Risk MJ, Hillaire-Marcel C, Tubrett M, Slyvester P, McCulloch M, Kinsley L (2005) Testing the reproducibility of Mg/Ca profiles in the deep-water coral *Primnoa resedaeformis*: putting the proxy through its paces. In: Freiwald A, Roberts JM (eds) Cold-water corals and ecosystems. Springer, Heidelberg, pp 1039–1060

Smith JE, Risk MJ, Schwarcz HP, McConnaughey TA (1997) Rapid climate change in the North Atlantic during the Younger Dryas recorded by deep-sea corals. Nature 386:818–820

Stuiver M, Reimer PJ (1993) Extended $^{14}$C database and revised CALIB radiocarbon calibration program. Radiocarbon 35:215–230

Waelbroeck C, Duplessy J-C, Michel E, Labeyrie L, Paillard D, Duprat J (2001) The timing of the last deglaciation in North Atlantic climate records. Nature 412:724–727